

BOUNDARY LAYER FLOW PAST SYMMETRICAL AIRFOIL AT HIGH SUBSONIC SPEEDS

By
V. K. DOGRA



DEPARTMENT OF AERONAUTICAL ENGINEERING

INDIAN INSTITUTE OF TECHNOLOGY KANPUR

JANUARY, 1977

TH
A 5/1/66
TH
AE. 1/1977/M
D6796
AE
1977
M
DOG
BOU

BOUNDARY LAYER FLOW PAST SYMMETRICAL AIRFOIL AT HIGH SUBSONIC SPEEDS

**A Thesis Submitted
in Partial Fulfilment of the Requirements
for the Degree of
MASTER OF TECHNOLOGY**

**By
V. K. DOGRA**

2013

to the

**DEPARTMENT OF AERONAUTICAL ENGINEERING
INDIAN INSTITUTE OF TECHNOLOGY KANPUR
JANUARY, 1977**

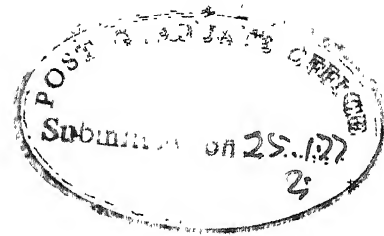
AE-1977-M-DCG-BOU

CEK

51160

Acc. No. 22

22 SEP 1977



CERTIFICATE

This is to certify that the work "BOUNDARY
LAYER FLOW PAST SYMMETRICAL AIRFOILS AT HIGH SUBSONIC
SPEEDS" has been carried out under my supervision and
has not been submitted elsewhere for a degree.

January 1977

N.L. Arora

(N.L. Arora)
Assistant Professor
Department of Aeronautical Engineering
Indian Institute of Technology
KANPUR.

RECEIVED OFFICE
THE INSTITUTE OF TECHNOLOGY
KANPUR
IN REPLY TO
regulations of the Indian
Institute of Technology Kanpur
Dated. Feb. 1. 1977

ACKNOWLEDGEMENTS

First and foremost, my deep and sincere gratitude goes to Dr. N.L. Arora, for several reasons, among them being excellent and invaluable guidance, continued encouragement through the long tort^uous work, and unfailing optimism.

I thank Mr. R.N. Srivastava for his neat and accurate typing.

Finally my unbounded thanks to my friends who helped me a lot at different stages of the work and during my stay at I.I.T. Kanpur.

January, 1977.

V.K. DOGRA

TABLE OF CONTENTS

	<u>Page</u>
SYNOPSIS	(iii)
NOMENCLATURE	(iv)
LIST OF FIGURES	(vii)
CHAPTER 1 INTRODUCTION	1
1.1 General	1
1.2 Literature Survey	2
1.3 Present Work	5
CHAPTER 2 PROBLEM FORMULATION	7
2.1 Boundary Layer Characteristics	8
2.2 Thin Airfoils in Boundary Layer Flow	11
CHAPTER 3 INTEGRAL EQUATION APPROACH	18
3.1 Introduction	18
3.2 Formulation of Integral Equation	19
3.3 Integral Equation for Perturbation Velocity Potential	25
3.4 Integral Equation for Perturbation Velocity for Non-lifting Case	26
3.5 Simplification of Integral Equation for Perturbation Velocity	29
3.6 Perturbation Velocity on the Surface of the Symmetrical Airfoil	31

	<u>Page</u>
CHAPTER 4 METHOD OF SOLUTION	34
4.1 Numerical Technique of Solution	34
4.2 Method of Iteration	36
4.3 Method of Parametric Differentiation	38
CHAPTER 5 COMPUTATIONAL DETAILS, RESULTS AND DISCUSSION	41
5.1 Introduction	41
5.2 Method of Iteration	41
5.3 Method of Parametric Differentiation	42
5.4 Results and Discussion	43
5.5 Conclusions	44
REFERENCES	46
APPENDIX A	48
APPENDIX B	
APPENDIX C	

SYNOPSIS

In the present work the symmetrical airfoil at zero incidence in high subsonic boundary layer flow has been considered. An airfoil in this kind of flow disturbs the boundary layer of flow field. The effect of perturbed boundary layer on the airfoil is incorporated by modifying its surface boundary conditions.

For high subsonic flows, the governing partial differential equation in terms of velocity perturbation velocity potential, which is non-linear, is transformed into an integral equation with the help of Green's theorem. Using functional relationship for velocity distribution the double integral is reduced to an integral valid on the surface of the airfoil. The integral equation is replaced by a set of non-linear algebraic equations by quadrature. The set of non-linear algebraic equations is solved by simple iteration. In the second method solution to this set of algebraic equations is obtained by applying the method of parametric differentiation. This results in first order non-linear differential equations. The set of ordinary differential equations is solved numerically by Hamming's Predictor-Corrector Method. The pressure distribution is obtained for some typical symmetrical airfoils at zero incidence.

NOMENCLATURE

a	-	Velocity of sound
A	-	Parameter defined by (4.2b)
A_1	-	Parameter defined by (3.3)
B	-	Parameter defined by (4.2b)
B_1	-	Parameter defined by (3.3)
c	-	Chord of the airfoil
C	-	Contour of the surface
C_p	-	Pressure coefficient
E	-	Kernel function of double integral defined by (3.30)
f	-	Parameter defining the surface of the airfoil
f_c	-	Parameter defining the camber of the airfoil
f_t	-	Thickness distribution of the airfoil
H	-	Shape factor defined by (2.2)
k	-	$(\gamma + 1)M_\infty^2$
M	-	Mach number
M_∞	-	Free stream Mach number
n	-	Normal to boundary surface
N	-	Number of intervals
R_c	-	Reynolds number
S	-	Boundary surface
u	-	Perturbation velocity in x-direction in normalised co-ordinate system
U	-	Perturbation velocity in X-direction in the physical co-ordinate system

u_L	-	Linear perturbation velocity in normalised plane
\bar{u}_L	-	Modified linear perturbation velocity
v	-	Perturbation velocity in y-direction in normalised plane
V	-	Perturbation velocity in Y-direction in physical plane
x, y	-	Normalised co-ordinates
X, Y	-	Physical system of co-ordinates
α	-	Angle of incidence
γ	-	Ratio of specific heats (= 1.4 for air)
ϵ_{ij}	-	Function defined in (4.2a)
ξ, ζ	-	Running co-ordinates in X, Y directions
θ	-	Momentum thickness defined by (2.2)
μ	-	Coefficient viscosity of fluid
$\bar{\mu}$	-	Artificial viscosity
ρ	-	Density
ρ_∞	-	Free stream density
ϕ	-	Normalised perturbation velocity potential
Φ	-	Perturbation velocity potential in physical plane
δ^*	-	Displacement thickness defined in (2.2)

Subscripts

c	-	Camber parameter
cr	-	Critical

e	-	Edge conditions of boundary layer
i,j	-	Values at different points on x-coordinate
l	-	Lower surface of the airfoil
L	-	Modified linear value
Ld	-	Modified linear value in physical plane
P	-	Singular point
t	-	Thickness parameter
u	-	Upper surface of the airfoil
w	-	Wall conditions
x,y	-	Partial derivatives with respect to x,y
X,Y	-	Partial derivatives with respect to X,Y
ξ,ζ	-	Partial derivatives with respect to ξ,ζ
∞	-	Free stream conditions
0,1	-	Mean and perturbation quantities

LIST OF FIGURES

1. Co-ordinate system and flow geometry
2. Domain of integration for Green's theorem
3. Flow chart for method of iteration
4. Flow chart for parametric differentiation method
5. Linear pressure distribution
6. Non-linear inviscid pressure distribution by two methods
7. Comparison of pressure distribution in boundary layer flow by two methods
8. Pressure distribution in boundary layer flow by method of iteration at $M_{\infty} = 0.4$
9. Pressure distribution in boundary layer flow by method of iteration at $M_{\infty} = 0.5$
10. Pressure distribution in boundary layer flow by method of iteration at $M_{\infty} = 0.6$
11. Pressure distribution in boundary layer flow by method of iteration at $M_{\infty} = 0.7$
12. Pressure distribution in boundary layer flow by method of iteration at $M_{\infty} = 0.72$

CHAPTER 1

INTRODUCTION

1.1 GENERAL

The problem of calculating the pressure distribution on a wing of given shape is of central importance in aeronautics. Generally the problem has been tackled considering the boundary layer on the airfoil or with the assumption of potential flow model. In the present work we calculate the pressure distribution on the airfoil ~~in~~ steady compressible boundary layer flow, rather than a potential flow model. More specifically, instead of assuming that the initial flow velocity is constant, we specify that it varies with the co-ordinate normal to wing surface, and increasing to a constant (free stream) value within a finite distance δ , from the wing. This type of initial flow is called boundary layer flow. The velocity profile within this region of boundary layer flow is chosen to resemble that observed in viscous turbulent boundary layer.

It is well-known that boundary layer flows are relatively more important for control surfaces than for the primary lifting surfaces. This type of flow is also created by some other agents, e.g., atmospheric boundary layer and propeller slip stream.

The pressure distribution on the surface of an airfoil in inviscid flow is determined by the airfoil geometry, i.e., the thickness distribution, the shape of the camber line and the incidence. In the case of symmetrical airfoil at zero incidence, the pressure distribution is dependent only on the thickness distribution. But an airfoil in the boundary layer flow disturbs the stream-lines close to the surface due to the perturbation of initial flow boundary layer. This is equivalent to a change in the thickness distribution. Thus airfoil surface is modified by adding perturbed boundary layer thickness or some kind of average perturbed boundary layer thickness, e.g., perturbed displacement thickness. This analysis becomes more complicated for super-critical flows, because of shock-wave boundary layer interaction on the surface of the airfoil.

1.2 LITERATURE SURVEY

The shear flow past airfoil and wavy shaped wall has been considered by several authors. Tsien (17) considered incompressible shear flow on symmetrical Joukowski airfoils. There, velocity distribution in shear layer far ahead from airfoil is assumed some kind of linear function. The linear governing equation in terms of stream function

is generated and solved for perturbation velocities with the help of usual boundary conditions of the airfoil flow. Lighthill (8) formulated steady compressible problem, deriving the inviscid perturbation equations and an asymptotic boundary condition. The appropriate boundary conditions are those of inviscid flow but with a mean boundary layer Mach number profile that goes to nonzero value at the wall. The incompressible problem for a stationary or travelling wavy wall has been treated by Benjamin (3) using full viscous perturbation equations. The effect of viscosity are included asymptotically near the wall. Inger and Williams (7) studied two dimensional steady compressible turbulent boundary layer flow past a slightly wavy wall, in subsonic and supersonic cases, both analytically and experimentally in the Mach number range $0.8 \leq M \leq 1.8$ at unit Reynolds numbers of the order of 10^6 per inch. The analysis is based on a parallel shear flow model of undisturbed boundary layer and linearized treatment of the small perturbation field, where the solution is decomposed into slowly varying inviscid part, which determines the pressure and a rapidly varying viscous part that is important near the wall. The measured and predicted wall pressure distributions are in good agreement. Yates (19) developed linearized integral theory of the viscous compressible flow past a wavy wall, in that

two integrals theories are derived for the calculation of pressure on a perturbed plane wall in a uniform main stream and in the presence of a viscous boundary layer. The integral theory may appropriately be called integral methods in that some kind of averaging over the thickness of boundary layer is employed. The first simple integral theory is derived from Von Kármán momentum integral equation (19) while the second rational integral theory is derived by iteration from the asymptotic perturbation theory. Both theories yield the same functional form for the wall pressure amplitude and phase angles in terms of a single similarity parameter, which is proportional to boundary layer thickness. The rational integral theory correlates better with experimental results than the simple theory. In recent years Ventres (18) presented a lifting surface theory based on a parallel shear flow model for steady, incompressible flows. The theory is intended to account approximately for the presence of a boundary layer. The method of Fourier transforms is used to calculate the pressure on a surface of infinite extent and arbitrary contour. Immediately above the surface is the region of sheared flow (the boundary layer), outside of which the flow velocity is constant. The Fourier transform of the pressure on this surface is used to derive the shear flow equivalent to the kernel function of

classical potential flow lifting surface theory. The kernel function provides an integral relation between upwash at a given point on the surface and pressure everywhere on the surface. It is found that shear layer decreases the lift curve slope; however, the shear layer (whose thickness is constant along the wing cord) has little effect on the centre of pressure.

Another approach to the wavy wall problem is to divide the shear layer into discrete increments of uniform potential flow. The problem of each layer is solved exactly and solutions for adjacent layers are matched. The limiting case of two layers was treated by Anderson and Fung (2). Zeydel (21) developed the theory for an arbitrary number of layers but did not present numerical results.

1.3 PRESENT WORK

The present work is an attempt to extend the integral method of Yates (19) for boundary layer flow past wavy wall at supersonic speeds to boundary layer flow past two dimensional airfoils at high subsonic speeds. In Chapter 2 the perturbed displacement thickness is evaluated by perturbing momentum integral equation of compressible boundary layer about mean boundary layer flow i.e. parallel

shear flow of the undisturbed boundary layer flow in terms of perturbation velocity. Then the airfoil surface is modified by adding the displacement thickness to it. In Chapter 3, following Oswatitsch-Gullstrand-Spreiter-Alksene approach the differential equation is transformed into an integral equation by the application of Green's theorem, for high-subsonic flow. Using functional relationship for velocity distribution, the double integral is reduced to an integral equation valid on the surface of the airfoil. In Chapter 4, the integral is converted to a system of non-linear algebraic equations. The solution to the integral equation is obtained by iteration scheme as well as by applying the method of parametric differentiation to the set of non-linear algebraic equations. Finally, results and discussion are given in Chapter 5. Some typical symmetrical profiles at zero incidence have been considered and pressure distribution is obtained at high subsonic speeds.

CHAPTER 2

PROBLEM FORMULATION

The method of treating airfoils in compressible boundary layer flows, is presented here. It may appropriately be called integral method in that some kind of averaging over thickness of boundary layer is employed. The analysis is based on a parallel shear flow model of undisturbed boundary layer, which is called mean boundary layer and perturbation boundary layer flow.

The approach is directly based on Von Kármán momentum integral equation and follows along the lines of Von Kármán-Pohlhausen technique (19) for calculating average boundary layer properties on airfoils, wind tunnel walls, etc. This type of integral approach has been developed and extended successfully by Lees (9) to more complicated flows that include, for example shock-wave boundary layer interaction. Also an attempt has been made by Yates (19) to use the integral theory for calculation of pressure on a wavy wall, in uniform main stream and in the presence of shear layer at steady supersonic speeds.

2.1 BOUNDARY LAYER CHARACTERISTICS

We assume steady compressible boundary layer flow of a perfect gas with unit Prandtl number, subjected to steady perturbations sufficiently small. Considering X-axis along the chord of the airfoil and Y-axis is directed normal to the chord as in Figure 1. Then momentum integral equation for compressible flows (13) can be written as:

$$\frac{d\theta}{dX} + \frac{\theta}{U_e} \cdot \frac{dU_e}{dX} (2 + H - M^2) = \frac{\tau_w}{\rho_e U_e^2} \quad (2.1)$$

where U is velocity of fluid in the direction of X-axis, ρ is density and μ is coefficient of viscosity in the boundary layer; and M is Mach number at the edge of the boundary layer. The subscripts e, w denote the quantities at the edge of the boundary layer and on the surface of the airfoil, respectively. The other parameters are defined as:

$$\begin{aligned} \delta^* &= \int_0^{\infty} \left(1 - \frac{\rho U}{\rho_e U_e}\right) dY \\ \theta &= \int_0^{\infty} \frac{\rho U}{\rho_e U_e} \left(1 - \frac{U}{U_e}\right) dY \\ H &= \frac{\delta^*}{\theta} \\ \tau_w &= \mu_w \left. \frac{\partial U}{\partial Y} \right|_w \end{aligned} \quad (2.2)$$

where δ^* is the displacement thickness, θ the momentum thickness, H shape factor and τ_w wall stress. Also, from the momentum equation at the edge of the boundary layer, we have

$$U_e \frac{dU_e}{dX} = - \frac{1}{\rho_e} \frac{dp}{dX} \quad (2.3)$$

The main idea is to perturb (2.1) about the basic mean boundary layer flow. The mean boundary layer is plane parallel shear flow in the X -direction with uniform pressure p_∞ , and arbitrary lateral variations of density $\rho_0(Y)$, velocity $U_0(Y)$ and Mach number $M_0(Y)$. To do so, we introduce two assumptions. First, we neglect the direct perturbation of the wall stress in (2.1). Second, we assume that the shape factor, H , is constant for the perturbed as well as the mean boundary layer flow. Thus

$$H\theta_0 = \delta_0^* \quad (2.4)$$

and

$$H(\theta_0 + \theta_1) = \delta_0^* + \delta_1^*$$

where the subscripts 0, 1 denote mean and perturbation quantities respectively. It follows from (2.4) that

$$\theta_1 = \frac{1}{H} \delta_1^* \quad (2.5)$$

In the absence of perturbations, (2.1) becomes

$$\frac{d\theta_o}{dX} = \frac{\tau_w}{\rho_e U_e^2} \quad (2.6)$$

Subtracting (2.6) from (2.1), we get

$$\frac{1}{H} \frac{d\delta_1^*}{dX} + \frac{\theta_o}{U_\infty} \frac{dU_e}{dX} (H + 2 - M_\infty^2) = 0 \quad (2.7)$$

Introducing pressure coefficient, we obtain from (2.3)

$$\frac{1}{U_\infty} \frac{dU_e}{dX} = -\frac{1}{2} \frac{dC_p}{dX} \quad (2.8)$$

where

$C_p = (p - p_\infty)/\frac{1}{2} \rho_\infty U_\infty^2$, p_∞ being the free stream static pressure. Using (2.8) into (2.7) we finally obtain

$$\frac{d\delta_1^*}{dX} = \frac{\delta_o^*}{2} [2 + H - M_\infty^2] \frac{dC_p}{dX} \quad (2.9)$$

Integrating (2.9), we obtain

$$\delta_1^* = \frac{\delta_o^*}{2} [H + 2 - M_\infty^2] C_p$$

This demonstrate simple proportionality between the perturbation displacement thickness and pressure coefficient, a key result of the integral theory.

The mean displacement thickness δ_o^* and mean momentum thickness θ_o are assumed equivalent to flat plate values at zero incidence and at fixed Reynolds numbers based on the chord of the airfoil. These are evaluated

according to method given by Stratford and Beavers (14) on the flat plate. In this method the $\frac{1}{7}$ th power law for velocity profile in turbulent compressible boundary layer is used for computing the values of δ_o^* and θ_o . The following set of results are obtained for free-stream Reynolds number R_c , of the order of 10^6

$$\begin{aligned}\delta_o^* &= 0.046(1 + 0.8M_\infty^2)^{0.44} c R_c^{-1/5} \\ \theta_o &= 0.036(1 + \frac{M_\infty^2}{10})^{-0.70} c R_c^{-1/5}\end{aligned}\tag{2.10}$$

and $H = \delta_o^*/\theta_o$

where M_∞ is the free stream Mach number and c is chord of the airfoil. For free-stream Reynolds number R_c , of the order of 10^7 the following are the results

$$\begin{aligned}\delta_o^* &= 0.028(1 + 0.8M_\infty^2)^{0.44} c R_c^{-1/6} \\ \theta_o &= 0.022(1 + \frac{M_\infty^2}{10}) c R_c^{-1/6}\end{aligned}\tag{2.11}$$

and $H = \delta_o^*/\theta_o$

2.2 THIN AIRFOILS IN BOUNDARY LAYER FLOW

A two dimensional cartesian co-ordinate system is chosen with the origin at the wing leading edge with

the X-axis in the free stream direction and Y-axis normal to free stream, as shown in Figure 1. The co-ordinates X and Y are scaled with respect to airfoil chord. A non-dimensional perturbation velocity potential, Φ , may be defined as

$$\Phi_X = \frac{\partial \Phi}{\partial X} = U, \quad \Phi_Y = \frac{\partial \Phi}{\partial Y} = V \quad (2.12)$$

where U and V are dimensionless perturbation velocities with respect to free stream velocity U_∞ , in X and Y direction respectively.

The equation of motion governing inviscid, non-heat conducting potential flow of a perfect gas around thin airfoils at transonic speeds can be written as (1)

$$[1 - M_\infty^2 - M_\infty^2 (\gamma + 1) \Phi_X] \Phi_{XX} + \Phi_{YY} = 0 \quad (2.13)$$

The upper and lower surfaces of the airfoil may be expressed as (Figure 1)

$$f_u = f_t(X) + f_c(X) - \alpha X \quad (2.14)$$

(upper surface)

$$(2.14)$$

$$f_l = -f_t(X) + f_c(X) - \alpha X$$

(lower surface)

where the body shape f is made dimensionless with respect to chord of the airfoil; $f_t(X)$ represents wing thickness

distribution, $f_c(X)$ is equation for the camber surface and α is airfoil angle of incidence.

The pressure coefficient $C_p(X, Y)$ can be evaluated by using Bernoulli's equation, thus

$$C_p(X, Y) = \frac{2}{\gamma M_\infty^2} \left[\left\{ 1 + \frac{\gamma-1}{2} M_\infty^2 (1 - q^2(X, Y)) \right\}^{\frac{\gamma}{\gamma-1}} - 1 \right] \quad (2.15a)$$

where γ is the ratio of specific heats ($\gamma = 1.4$) and, $q(X, Y)$, is defined as

$$q(X, Y) = [(1 + \Phi_X^2) + \Phi_Y^2]^{1/2} \quad (2.15b)$$

A first order approximation to pressure coefficient consistent with (2.13) is given by

$$C_p(X, Y) = -2\Phi_X(X, Y) \quad (2.16a)$$

which on the surface of the airfoil reduces to

$$C_p(X, 0_\pm) = -2\Phi_X(X, 0_\pm) \quad (2.16b)$$

The complete problem for the perturbation field can now be expressed as follows. Following second-order boundary layer theory (16), we solve for the inviscid flow subject to the boundary condition, on the airfoil surface plus the displacement thickness, i.e.

$$Y = f + \delta_1^*/c \quad (2.17)$$

where c is chord of the airfoil. Thus, we must solve (2.13) subject to the boundary condition in the plane of the airfoil ($Y = 0_{\pm}$) which can be expressed as

$$\frac{\partial \Phi}{\partial Y}(X, 0_{\pm}) = \pm \frac{df}{dX} \pm \frac{1}{c} \frac{\partial \delta_1^*}{\partial X} \quad (2.18a)$$

using (2.9) together with (2.16b), we obtain from (2.18a)

$$\frac{\partial \Phi}{\partial Y}(X, 0_{\pm}) = \pm \frac{df}{dX} \mp \left[\frac{\delta_0^*}{c} (H + 2 - M_{\infty}^2) \right] \Phi_{XX}(X, 0_{\pm}) \quad (2.18b)$$

In addition following conditions are to be satisfied.

All the disturbances produced by the airfoil must die out uniformly with increasing distance away both from the airfoil and any downstream wake that may trail behind it i.e., at infinity

$$\Phi_X \text{ and } \Phi_Y \rightarrow 0 \quad (2.19)$$

For lifting surfaces, it is necessary that Φ_X and Φ_Y remain continuous and finite at the trailing edges i.e. Kutta condition is satisfied.

It should be noted that (2.13) describes correctly small perturbation in subsonic as well as supersonic flows, because then nonlinear term becomes negligible. The type of equation is dependent on the sign of the coefficient of Φ_{XX} , as follows

$$[1 - M_{\infty}^2 - M_{\infty}^2 (\gamma + 1) \Phi_X] \begin{cases} > 0 & \text{elliptic (subsonic)} \\ = 0 & \text{parabolic (sonic)} \\ < 0 & \text{hyperbolic (supersonic)} \end{cases}$$

The above coefficient is equivalent in the high subsonic flow theory to $(1 - M^2)$, where M is the local Mach number. The critical value of $U = \Phi_X$ associated with $M = 1$ is thus

$$U_{cr} = \frac{1 - M_{\infty}^2}{(\gamma + 1) M_{\infty}^2}$$

The lowest free stream Mach number corresponding to which the local Mach number becomes unity on the surface of the airfoil is called the critical Mach number. The flow with free stream Mach number less than critical value is called the subcritical flow, and the flow with free stream Mach number higher than critical value is called the supercritical flow. The supercritical flow in general is not shock free. Hence while treating supercritical flow, we have to take the effect of shock wave boundary layer interaction, which makes the problem much more complicated than the subcritical. However, we have considered here only transonic viscous subcritical flows.

The steady small disturbance supersonic potential equation of inviscid, non-conducting isentropic flow around two dimensional airfoil is obtained by neglecting the nonlinear term in (2.13), we obtain

$$\Phi_{XX} - \frac{1}{\lambda^2} \Phi_{YY} = 0 \quad (2.20)$$

where $\lambda = \sqrt{M_\infty^2 - 1}$

The equation (2.20) is hyperbolic and it can be solved subject to the boundary condition (2.18b) in the plane of the airfoil ($Y = 0_\pm$) and in addition boundary condition at infinity (2.19).

The general solution of hyperbolic equation (2.20) is given by

$$\Phi = F(X - \lambda Y) \quad (2.21)$$

For the perturbation velocity components on the surface of the airfoil, we have

$$\begin{aligned} \Phi_X(X, 0_\pm) &= F' \\ \Phi_Y(X, 0_\pm) &= -\lambda F' \end{aligned} \quad (2.22)$$

Using (2.22) and (2.16b) in the surface boundary condition of the airfoil (2.18b)

$$\frac{\lambda}{2} c_p(X, 0_\pm) = \pm \frac{df}{dX} \pm \frac{\delta_o^*}{2c} (H + 2 - M_\infty^2) \frac{dc_p}{dX}(X, 0_\pm)$$

or

$$-\frac{\delta_o^*}{c} (H + 2 - M_\infty^2) \frac{dc_p(X, 0)}{dX} + c_p(X, 0) = 2 \frac{df}{dX} \quad (\text{for the upper surface})$$

$$\frac{\delta_o^*}{c} (H + 2 - M_\infty^2) \frac{dc_p(X, 0-)}{dX} - c_p(X, 0-) = -2 \frac{df}{dX} \quad (2.23)$$

(for the lower surface)

Equation (2.23) is simple first-order differential equation for surface pressure coefficient.

In the absence of any boundary layer, we see that (2.23) reduces to the usual inviscid result

$$C_p = \frac{2}{\lambda} \frac{df}{dX} \quad (\text{inviscid})$$

The general solution for (2.23) can be written as

$$\begin{aligned} C_p &= \frac{4\pi}{|\lambda|\chi} \int_X^\infty e^{-\frac{2\pi\lambda}{|\lambda|\chi}(\xi - X)} \frac{df}{d\xi} d\xi \quad M_\infty < M_c \\ &= -\frac{4\pi}{|\lambda|\chi} \int_\infty^X e^{-\frac{2\pi\lambda}{|\lambda|\chi}(\xi - X)} \frac{df}{d\xi} d\xi \quad M_\infty > M_c \\ \chi &= \frac{2\pi}{|\lambda|} \frac{\delta_o^*}{c} (M_c^2 - M_\infty^2) \end{aligned}$$

where $M_c = (H + 2)^{\frac{1}{2}}$.

CHAPTER 3

INTEGRAL EQUATION APPROACH

3.1 INTRODUCTION

To find the pressure distribution around wing in high-subsonic boundary layer flow, we adopt the integral equation method. The integral equation approach for inviscid transonic flows has been developed by Ostwatitsch (12), Gullstrand (6), and Spreiter and Alksne (15). Recently this approach has been further worked out and refined by Norstrud (11) and Nixon and Hancock (10).

In this approach the application of Green's theorem transforms the governing non-linear partial differential equation into an integral equation. That gives the perturbation velocity potential at a general point in the flow field, in terms of a line integral of linear function of the velocity potential around the airfoil surface and a double (surface) integral of non-linear term. For the perturbation velocity potential in the plane of the airfoil, this double integral is reduced to the simple line integral.

3.2 FORMULATION OF INTEGRAL EQUATION

3.2.1 Transformation

It is convenient to introduce the following transformation

$$\begin{aligned}\phi &= \frac{M_\infty^2 (\gamma + 1)}{(1 - M_\infty^2)} \Phi \\ x &= X \\ y &= (1 - M_\infty^2)^{1/2} Y\end{aligned}\tag{3.1}$$

Substituting (3.1) into (2.13), (2.18b) and (2.19), the problem of boundary layer flow past airfoils at high subsonic speed is reduced to finding the solution of the equation

$$\phi_{xx} + \phi_{yy} = \phi_x \phi_{xx}\tag{3.2}$$

together with the following boundary conditions.

In the plane of the airfoil

$$\phi_y(x, 0_\pm) = \pm A_1 \frac{df}{dx} + B_1 \phi_{xx}(x, 0_\pm)$$

where

$$\begin{aligned}A_1 &= \frac{(\gamma + 1) M_\infty^2}{(1 - M_\infty^2)^{3/2}} \\ \text{and} \\ B_1 &= \frac{\left[\frac{\delta_0^*}{c} (H + 2 - M_\infty^2) \right]}{(1 - M_\infty^2)^{1/2}}\end{aligned}\tag{3.3}$$

At infinity, $\phi_x, \phi_y \rightarrow 0$

ϕ_x, ϕ_y are finite and continuous at the trailing edge (Kutta condition).

The pressure coefficient in the transformed plane is obtained from

$$C_p(x, 0_{\pm}) = - \frac{2(1 - M_{\infty}^2)}{(\gamma + 1) M_{\infty}^2} \phi_x(x, 0_{\pm})$$

3.2.2 Application of Green's Theorem

The equation (3.2) may be transformed into an integral equation by application of Green's theorem.

If $\sigma(x,y)$ and $\Omega(x,y)$ are two continuous functions with continuous first and second derivatives in some domain S , bounded by curve C , then Green's theorem states

$$\begin{aligned} \iint_S [\Omega(x,y) \nabla^2 \sigma(x,y) - \sigma(x,y) \nabla^2 \Omega(x,y)] dS \\ = - \int_C [\Omega(x,y) \frac{\partial \sigma(x,y)}{\partial n} - \sigma(x,y) \frac{\partial \Omega(x,y)}{\partial n}] dC \end{aligned} \quad (3.4)$$

where ∇^2 is Laplacian operator $(\frac{\partial^2}{\partial x^2} + \frac{\partial^2}{\partial y^2})$, and where, n , is inward drawn normal to curve C around which the integration must be considered in an anticlockwise direction.

In (3.4) let $\sigma(x,y)$ be identified with perturbation velocity potential ϕ , so that (3.2) gives

$$\begin{aligned}
\nabla^2 \sigma(x,y) &\equiv \nabla^2 \phi(x,y) = \phi_{xx} \\
&= \frac{\partial}{\partial x} (\phi_x^2/2) \\
&= \frac{\partial}{\partial x} (u^2/2)
\end{aligned} \tag{3.5}$$

Again $\Omega(x,y)$ is chosen as the elementary source solution of Laplace's equation

$$\nabla^2 \Omega = 0 \tag{3.6a}$$

$$\text{i.e. } \Omega(x, \xi; y, \zeta) = \ln(r) \tag{3.6b}$$

where $r = [(x - \xi)^2 + (y - \zeta)^2]^{1/2}$, with ξ and ζ being the running co-ordinates in x and y directions respectively.

Now $\Omega(x, y; \xi, \zeta)$ is singular at the point $P(x,y)$. Also to the present order of approximation, $\phi(\xi, \zeta)$ and its derivatives can be discontinuous across the slit ($0 \leq \xi \leq 1$, $\zeta = 0_{\pm}$) on the ξ -axis, where the boundary conditions are to be applied. Since $\Omega(x, y; \xi, \zeta)$ and $\phi(x,y)$, and their derivatives must be continuous throughout the domain S , the point $P(x,y)$ and slit ($0 \leq \xi \leq 1$, $\zeta = 0_{\pm}$) must be excluded from S . This domain is shown in Figure 2.

On substituting (3.5) and (3.6) in (3.4), we obtain

$$\begin{aligned}
& \iint_S \Omega(x, \xi; y, \zeta) - \frac{\partial}{\partial \xi} \left(\frac{u^2}{2} \right) (\xi, \zeta) ds \\
&= - \int_{C_1 + C_W + C_\infty} \left[\Omega(x, \xi; y, \zeta) \frac{\partial \phi}{\partial n} - \phi(\xi, \zeta) \frac{\partial \Omega(x, \xi; y, \zeta)}{\partial n} \right] dC
\end{aligned} \tag{3.7}$$

where C_1 is the part of the boundary C surrounding the point $P(x, y)$ and is taken to be small circle of radius r_p . C_W is that part of the boundary C surrounding the ξ -axis, and C_∞ completes the boundary C , thus denoting the outer limiting boundary of S , taken to be a large circle, centre at the origin, of radius R . These boundaries C_1 , C_W , C_∞ together with the sense of integration, are shown in Figure 2. The integral over surface S can be obtained directly without mentioning any surface distribution, but for line integral each boundary will be considered separately.

3.2.3 Integral Over Boundary C

- (i) Integral over boundary C_1 surrounding the singular point P :

The radius of circle surrounding the point $P(x, y)$ is r_p and so

$$\delta C = r_p \delta \theta$$

taking θ to increase in clockwise direction. Since

$$\Omega(x, y; \xi, \zeta) = \ln(r_p)$$

$$\frac{\partial}{\partial n} = \frac{\partial}{\partial r_p}$$

and

$$\begin{aligned} \frac{\partial \Omega(x, y; \xi, \zeta)}{\partial n} &= \frac{\partial}{\partial r_p} (\ln r_p) \\ &= + \frac{1}{r_p} \end{aligned}$$

Thus, the integration over C_1 , in limiting operation as $r_p \rightarrow 0$ is written as

$$\begin{aligned} \lim_{r_p \rightarrow 0} \int_{C_1} [\ln(r_p) \frac{\partial \phi(\xi, \zeta)}{\partial n} - \phi(\xi, \zeta) \frac{\partial}{\partial n} (\ln(r_p))] dC \\ = - \lim_{r_p \rightarrow 0} \phi \int_0^{2\pi} \frac{1}{r_p} \cdot r_p d\theta \\ = - 2\pi \phi(x, y) \end{aligned} \quad (3.8)$$

because all terms in line integral over C_1 vanish except those, involving derivatives of $\Omega(x, y; \xi, \zeta)$, as $r_p \rightarrow 0$.

(ii) Integral over boundary C_w :

For thin airfoil with thin boundary layer on its surface, we can write

$$\frac{\partial}{\partial n} = \pm \frac{\partial}{\partial \zeta} \quad \text{on the plane of the wing}$$

Thus

$$\begin{aligned}
 & \int_{C_w} [\Omega(x, \xi; y, \zeta) \frac{\partial \phi(\xi, \zeta)}{\partial n} - \phi(\xi, \zeta) \frac{\partial \Omega(x, \xi; y, \zeta)}{\partial n}] d\zeta \\
 &= \int_0^\infty [\Omega(x, \xi; y, 0) \Delta \frac{\partial \phi(\xi, 0)}{\partial \zeta} \\
 &\quad - \Delta \phi(\xi, 0) \frac{\partial \Omega(x, \xi; y, 0)}{\partial \zeta}] d\xi \quad (3.9)
 \end{aligned}$$

where

$$\begin{aligned}
 \Delta \phi(\xi, 0) &= \phi(\xi, 0+) - \phi(\xi, 0-) \\
 \Delta \frac{\partial \phi(\xi, 0)}{\partial \zeta} &= \Delta \frac{\partial \phi(\xi, 0)}{\partial \zeta} = \frac{\partial \phi(\xi, 0+)}{\partial \zeta} - \frac{\partial \phi(\xi, 0-)}{\partial \zeta}
 \end{aligned}$$

(iii) Integral over boundary C_∞ :

For integral over C_∞ , the perturbation velocity potential $\phi(\xi, \zeta)$ will be of the form $\phi(\xi, \zeta) = O(\theta + \frac{1}{R})$ for a lifting airfoil (for non-lifting airfoil the θ term should be omitted), where (R, θ) are the polar co-ordinates on C_∞ . Thus the line integral over C_∞ is a constant for lifting airfoil. Then

$$\begin{aligned}
 & \int_C [\Omega(x, \xi; y, \zeta) \frac{\partial \phi(\xi, \zeta)}{\partial n} - \phi(\xi, \zeta) \frac{\partial \Omega(x, \xi; y, \zeta)}{\partial n}] d\zeta \\
 &= \text{Constant (for lifting case)} \\
 &= 0 \quad (\text{for non-lifting case}) \quad (3.10)
 \end{aligned}$$

This constant is equal to the strength of circulation around the airfoil and exact value of this constant is

immaterial since it will disappear in the application of a differential operator.

3.3 INTEGRAL EQUATION FOR PERTURBATION VELOCITY POTENTIAL

Now substituting (3.8), (3.9) and (3.10) in (3.7), we get

$$\begin{aligned} \phi(x,y) = & \frac{1}{2\pi} \int_0^\infty [\Omega(x,\xi; y,0) \Delta \phi(\xi,0) - \Omega(x,\xi; y,0) \Delta \phi(\xi,0)] d\xi \\ & + \frac{1}{2\pi} \iint_S \Omega(x,y; \xi, \zeta) \frac{\partial}{\partial \xi} \left(\frac{u^2}{2}(\xi, \zeta) \right) dS + \text{Constant} \quad (3.11) \end{aligned}$$

The surface integral in (3.11) can be defined in the same fashion as given by Spreiter and Alksne (15). Thus for field points in the upper half plane ($y > 0$)

$$\begin{aligned} \iint_S F dS = & \lim_{\epsilon \rightarrow 0} \left\{ \int_0^\infty \left(\int_{-\infty}^{x-\epsilon} F d\xi \right) d\zeta + \int_0^\infty \left(\int_{x+\epsilon}^\infty F d\xi \right) d\zeta \right. \\ & \left. + \int_{-\infty}^0 \left(\int_{-\infty}^\infty F d\xi \right) d\zeta \right\} \quad (3.12) \end{aligned}$$

and for lower half plane ($y < 0$)

$$\begin{aligned} \iint_S F dS = & \lim_{\epsilon \rightarrow 0} \left\{ \int_0^\infty \left(\int_{-\infty}^\infty F d\xi \right) d\zeta + \int_{-\infty}^0 \left(\int_{-\infty}^{x-\epsilon} F d\xi \right) d\zeta \right. \\ & \left. + \int_{-\infty}^0 \left(\int_{x+\epsilon}^\infty F d\xi \right) d\zeta \right\} \end{aligned}$$

The double integral in (3.11) can be integrated by parts with respect to ξ , so that

$$\begin{aligned}
\phi(x,y) = & \frac{1}{2\pi} \int_0^{\infty} [\Omega(x, \xi; y, 0) \Delta \phi_{\zeta}(\xi, 0) - \\
& \Omega_{\zeta}(x, \xi; y, 0) \Delta \phi(\xi, 0)] d\xi \\
& - \frac{1}{2\pi} \iint_S \Omega_{\xi}(x, \xi; y, \zeta) \frac{u^2}{2}(\xi, \zeta) dS + \text{Constant}
\end{aligned} \tag{3.13}$$

$$\text{where } \Omega(x, y; \xi, \zeta) = \ln [(x - \xi)^2 + (y - \zeta)^2]^{\frac{1}{2}}$$

3.4 INTEGRAL EQUATION FOR PERTURBATION VELOCITY FOR NON-LIFTING CASE

In the symmetrical flow problem in the plane of the wing ($y = 0_{\pm}$)

$$\phi(x, 0+) = \phi(x, 0-)$$

$$\text{so that } \Delta \phi = 0 \tag{3.14}$$

$$\text{and } \frac{\partial \phi(x, 0+)}{\partial y} = - \frac{\partial \phi(x, 0-)}{\partial y}$$

Thus we obtain from (3.13)

$$\begin{aligned}
\phi(x,y) = & \frac{1}{2\pi} \int_0^{\infty} \ln [(x - \xi)^2 + y^2]^{\frac{1}{2}} \Delta \phi_{\zeta} d\xi - \frac{1}{2\pi} \iint_S \frac{u^2}{2}(\xi, \zeta) \Omega_{\xi} \\
& \tag{3.15}
\end{aligned}$$

$$\text{with } u = \phi_x$$

Now differentiating (3.15) with respect to x , we obtain for $\phi_x(x, y)$ or $u(x, y)$

$$\begin{aligned}
u(x,y) &= \frac{1}{\pi} \int_0^{\infty} \frac{(x - \xi)}{[(x - \xi)^2 + y^2]} \Delta \phi(\xi, 0) d\xi \\
&+ \frac{u^2}{2}(x,y) - \frac{1}{2\pi} \iint_S \frac{u^2(\xi, \zeta)}{2} \frac{[(x - \xi)^2 - (y - \zeta)^2]}{[(x - \xi)^2 + (y - \zeta)^2]^2} d\xi d\zeta
\end{aligned} \tag{3.16}$$

The term $\frac{u^2}{2}(x,y)$ arises from the differentiation of the limits around the singular point $P(x,y)$ in the surface integral. The boundary condition (3.3), for symmetrical airfoil gives

$$\frac{\partial \phi(x,0)}{\partial y} = A_1 \frac{df_t}{dx} - B_1 \frac{\partial u(x,0)}{\partial x} \tag{3.17}$$

Substituting (3.17) in (3.16), we get

$$\begin{aligned}
u(x,y) &= \frac{A_1}{\pi} \int_0^{\infty} \frac{df_t}{d\xi} \frac{(x - \xi)}{[(x - \xi)^2 + y^2]} d\xi \\
&- \frac{B_1}{\pi} \int_0^{\infty} \frac{\partial u(\xi, 0)}{\partial \xi} \frac{(x - \xi)}{[(x - \xi)^2 + y^2]} d\xi + \frac{u^2}{2}(x,y) \\
&- \frac{1}{2\pi} \iint_S \frac{u^2(\xi, \zeta)}{2} \frac{[(x - \xi)^2 - (y - \zeta)^2]}{[(x - \xi)^2 + (y - \zeta)^2]^2} d\xi d\zeta
\end{aligned} \tag{3.18}$$

The equation (3.18) can also be written as

$$u(x,y) = u_L(x,y) - u_S(x,y) + \frac{u^2}{2}(x,y) - I(x,y) \tag{3.19}$$

where

$$u_L(x,y) = \frac{A_1}{\pi} \int_0^{\infty} \frac{df_t}{d\xi} \frac{(x - \xi)}{[(x - \xi)^2 + y^2]} d\xi \quad (3.20a)$$

is essentially the linear perturbation velocity,

$$u_S(x,y) = \frac{B_1}{\pi} \int_0^{\infty} \frac{du(\xi,0)}{d\xi} \frac{(x - \xi)}{[(x - \xi)^2 + y^2]} d\xi \quad (3.20b)$$

is the boundary layer contribution, and

$$I = \frac{1}{2\pi} \iint_S \frac{u^2}{2}(\xi, \zeta) \frac{(x - \xi)^2 - (y - \zeta)^2}{[(x - \xi)^2 + (y - \zeta)^2]^2} d\xi d\zeta \quad (3.20c)$$

is the non-linear contribution. The integral $u_S(x,y)$ can be further simplified by integrating by parts, thus

$$u_S(x,y) = \frac{B_1}{\pi} \left\{ \frac{(x - \xi)}{[(x - \xi)^2 + y^2]} u(\xi,0) \Big|_0^{\infty} - \int_0^{\infty} u(\xi,0) \frac{[(x - \xi)^2 - y^2]}{[(x - \xi)^2 + y^2]^2} d\xi \right\}$$

It is assumed that the perturbation flow ahead of and behind the airfoil has very small effect on the values of $u_S(x,y)$, hence the first term in above integral can be neglected. Thus

$$u_S(x,y) \simeq - \frac{B_1}{\pi} \int_0^{\infty} u(\xi,0) \frac{[(x - \xi)^2 - y^2]}{[(x - \xi)^2 + y^2]^2} d\xi \quad (3.20d)$$

Now from (3.18), (3.19) and (3.20d), we get

$$\begin{aligned}
 u(x,y) = & \frac{A_1}{\pi} \int_0^{\infty} \frac{df_t}{d\xi} \frac{(x - \xi)}{[(x - \xi)^2 + y^2]} d\xi + \\
 & \frac{B_1}{\pi} \int_0^{\infty} u(\xi, 0) \frac{[(x - \xi)^2 - y^2]}{[(x - \xi)^2 + y^2]^2} d\xi + \frac{u^2}{2}(x,y) \\
 & - \frac{1}{2\pi} \iint_S \frac{u^2(\xi, \zeta)}{2} \frac{[(x - \xi)^2 - (y - \zeta)^2]}{[(x - \xi)^2 + (y - \zeta)^2]^2} d\xi d\zeta
 \end{aligned} \tag{3.21}$$

3.5 SIMPLIFICATION OF INTEGRAL EQUATION FOR PERTURBATION VELOCITY

In solving (3.21) the difficulty arises due to the kernel of double integral. Therefore before proceeding further the kernel of double integral and hence integral equation is simplified. Following Spreiter and Alksne (15) a functional relationship

$$u(x,y) = \frac{u(x,0^{\pm})}{[1 \pm \frac{y}{b(x)}]^2} \tag{3.22}$$

is assumed between the velocity on the airfoil surface and the velocity directly above the surface of the airfoil. The expression (3.22) satisfies the boundary condition of zero disturbance at $\pm\infty$. The parameter $b(x)$ is found by using the condition of irrotationality and the boundary condition

(3.3); Differentiating (3.22) with respect to y and setting $y = 0_{\pm}$, we have

$$b(x) = - \frac{2u(x, 0_{\pm})}{\left. \frac{\partial u}{\partial y} \right|_{y=0_{\pm}}} \quad (3.23)$$

From the irrotationality condition

$$\left. \frac{\partial u}{\partial y} \right|_{y=0_{\pm}} = \left. \frac{\partial v}{\partial x} \right|_{y=0_{\pm}} \quad (3.24)$$

The boundary condition (3.3) gives

$$\left. \frac{\partial v}{\partial x} \right|_{y=0_{\pm}} = \pm A_1 \frac{d^2 f}{dx^2} \mp B_1 \frac{\partial^2 u}{\partial x^2}(x, 0_{\pm}) \quad (3.25)$$

Substituting (3.24) and (3.25) into (3.23), we get

$$b(x) = \frac{-2u(x, 0_{\pm})}{\frac{(\gamma+1)M_{\infty}^2}{(1-M_{\infty}^2)^{3/2}} \left[\frac{d^2 f}{dx^2} \mp \left\{ \frac{\delta_0^*}{c} (H+2-M_{\infty}^2) \right\} \frac{(1-M_{\infty}^2)}{(\gamma+1)M_{\infty}^2} \frac{\partial^2 u(x, 0_{\pm})}{\partial x^2} \right]}$$

The typical calculation shows that $\frac{\delta_0^*}{c} (H+2-M_{\infty}^2) \sim 0(10^{-3})$. This when multiplied with $\frac{\partial^2 u}{\partial x^2}$ (which is of the same order of magnitude as $\frac{d^2 f}{dx^2}$) becomes one order higher as compared with the first term in the denominator, and therefore can be neglected. Thus

$$b(x) \simeq - \frac{2u(x, 0_{\pm})(1-M_{\infty}^2)^{3/2}}{(\gamma+1)M_{\infty}^2 \frac{d^2 f}{dx^2}} \quad (3.26)$$

3.6 PERTURBATION VELOCITY ON THE SURFACE OF THE SYMMETRICAL AIRFOIL

Substituting relation (3.26) into (3.21), we obtain

at $y = 0$

$$\begin{aligned}
 u(x,0) &= \frac{A_1}{\pi} \int_0^\infty \frac{df_t}{d\xi} \frac{d\xi}{(x-\xi)} + \frac{B_1}{\pi} \int_0^\infty u(\xi,0) \frac{d\xi}{(x-\xi)^2} \\
 &+ \frac{u^2(x,0)}{2} - \frac{1}{2\pi} \iint_{-\infty}^\infty \frac{u^2(\xi,0\pm)}{2} \frac{[(x-\xi)^2 - \zeta^2]}{[(x-\xi)^2 + \zeta^2]^2} \\
 &\quad \frac{d\xi d\zeta}{[1 \pm \frac{\zeta}{b}]^2} \\
 &= \frac{A_1}{\pi} \int_0^\infty \frac{df_t}{d\xi} \frac{d\xi}{(x-\xi)} + \frac{B_1}{\pi} \int_0^\infty u(\xi,0) \frac{d\xi}{(x-\xi)^2} + \frac{u^2(x,0)}{2} \\
 &- \frac{1}{2\pi} \int_{-\infty}^\infty \left[\int_{-\infty}^0 \frac{u^2(\xi,0-)}{2} \frac{[(x-\xi)^2 - \zeta^2]}{[(x-\xi)^2 + \zeta^2]^2} \frac{d\zeta}{(1 - \frac{\zeta}{b})^2} \right. \\
 &\quad \left. + \int_0^\infty \frac{u^2(\xi,0)}{2} \frac{[(x-\xi)^2 - \zeta^2]}{[(x-\xi)^2 + \zeta^2]^2} \frac{d\zeta}{(1 + \frac{\zeta}{b})^2} \right] d\xi \quad (3.27)
 \end{aligned}$$

Since the airfoil is symmetrical, we have

$$u(\xi,0+) = -u(\xi,0-) \quad (3.28)$$

Using (3.28) in (3.27), we get

$$\begin{aligned}
u(x,0) = & \frac{A_1}{\pi} \int_0^{\infty} \frac{df_t}{d\xi} \frac{d\xi}{(x-\xi)} + \frac{B_1}{\pi} \int_0^{\infty} u(\xi,0) \frac{d\xi}{(x-\xi)^2} \\
& + \frac{u^2}{2}(x,0) - \frac{1}{2\pi} \int_{-\infty}^{\infty} \left[\int_0^{\infty} u^2(\xi,0) \frac{(x-\xi)^2 - \zeta^2}{[(x-\xi)^2 + \zeta^2]^2} \right. \\
& \left. \frac{d\zeta}{(1 + \frac{\zeta}{b})^2} \right] d\xi \quad (3.29)
\end{aligned}$$

The (3.29) is further simplified as

$$\begin{aligned}
u(x,0) = & \frac{A_1}{\pi} \int_0^{\infty} \frac{df_t}{d\xi} \frac{d\xi}{(x-\xi)} + \frac{B_1}{\pi} \int_0^{\infty} u(\xi,0) \frac{d\xi}{(x-\xi)^2} \\
& + \frac{u^2}{2}(\xi,0) - \int_{-\infty}^{\infty} \frac{u^2(\xi,0)}{2b(\xi)} E(Z) d\xi \quad (3.30)
\end{aligned}$$

where $E(Z) \equiv E\left(\frac{|x-\xi|}{b}\right)$

$$= \frac{1}{\pi} \int_0^{\infty} \frac{(x-\xi)^2 - \zeta^2}{[(x-\xi)^2 + \zeta^2]^2} \frac{b}{[1 + \frac{\zeta}{b}]^2} d\zeta$$

Now writing (3.30) as below

$$u(x,0) = u_L(x,0) + u_S(x,0) + \frac{u^2}{2}(x,0) - I(x,0) \quad (3.31)$$

where

$$u_L(x,0) = \frac{A_1}{\pi} \int_0^{\infty} \frac{df_t}{d\xi} \frac{d\xi}{(x-\xi)} \quad (3.32a)$$

The linear perturbation velocity on the surface of the airfoil

$$u_s(x,0) = \frac{B_1}{\pi} \int_0^{\infty} u(\xi,0) \frac{d\xi}{(x-\xi)^2} \quad (\text{viscous contribution}) \quad (3.32b)$$

and

$$I(x,0) = \int_{-\infty}^{\infty} \frac{u^2(\xi,0)}{2b(\xi)} E(Z) d\xi \quad (\text{non-linear contribution}) \quad (3.32c)$$

The linear perturbation velocity $u_L(x,0)$ in (3.31) is singular at the leading edge for round nosed airfoils. Therefore, for more accurate solution this is corrected to new modified value $\bar{u}_L(x,0)$ (see Appendix A) as

$$\bar{u}_L(x,0) = \frac{\frac{k}{\beta_{\infty}^2} + u_L(x,0)}{\left[1 + \left(\frac{\beta_{\infty}^2}{k} \frac{df_t}{dx}\right)^2\right]^{\frac{1}{2}}} - \frac{k}{\beta_{\infty}^2}$$

where $k = (\gamma + 1) M_{\infty}^2$ and $\beta_{\infty} = \sqrt{1 - M_{\infty}^2}$

Thus, substituting this modified linear value in (3.31), we get

$$u(x,0) = \bar{u}_L(x,0) + u_s(x,0) + \frac{u^2}{2}(x,0) - I(x,0) \quad (3.33)$$

CHAPTER 4

METHOD OF SOLUTION

4.1 NUMERICAL TECHNIQUE OF SOLUTION

The integral equation (3.33) of Chapter 3 is solved by quadrature, by approximating the range of integration with a finite number N of discrete intervals and letting the unknown function $u = u(x,0)$ be represented by a mean value within each element. For points ahead of the leading edge ($x < 0$) or points aft of trailing edge ($x > 1$), the expression for u as given in (3.33) is going to be identically zero. Thus it is assumed that the influence of the points upstream and downstream of the profile on the value of $u(x,0)$ can be neglected. Thus (3.33) can be represented by the following system of non-linear algebraic equations.

$$u_i = \bar{u}_{L_i} + \frac{1}{2}u_i^2 - \sum_{j=1}^N \epsilon_{ij} u_j^2/2 + \sum_{j=1}^N \delta_{ij} u_j \quad (4.1)$$

$i = 1, 2, \dots, N$

where ϵ_{ij} and δ_{ij} are defined as (5)

$$\epsilon_{ij} = \int_{\xi_j - 1/2}^{\xi_j + 1/2} \int_{\xi_j - 1/2}^{\xi_j + 1/2} \left[\frac{x_i - \xi}{b(\xi)} \right] d\xi$$

$$\begin{aligned}
&= \frac{4}{\pi} \frac{1}{12(1+A^2)^4} \left\{ \frac{3\pi}{2} \frac{A}{|A|} [(1+A^2)^4 - (1+A^2)^2 + 8(1+A^2) - 8] \right. \\
&\quad \left. + 12A(A^2-1) \ln |A| - A(1+A^2) [(1+A^2) + 12] \right\} \\
&+ \frac{4}{\pi} \frac{1}{12(1+B^2)^4} \left\{ \frac{3\pi}{2} \frac{B}{|B|} [(1+B^2)^4 - (1+B^2)^2 + 8(1+B^2) - 8] \right. \\
&\quad \left. + 12B(B^2-1) \ln |B| - B(1+B^2) [(1+B^2) + 12] \right\} \quad (4.2a)
\end{aligned}$$

$$\left. \begin{aligned}
A &= \frac{1}{b_j} \left[\frac{l_j}{2} + (x_i - \xi_j) \right] \\
B &= \frac{1}{b_j} \left[\frac{l_j}{2} - (x_i - \xi_j) \right]
\end{aligned} \right\} \quad (4.2b)$$

and

$$\begin{aligned}
\delta_{ij} &= \int_{\xi_j - l_j/2}^{\xi_j + l_j/2} (x_i - \xi)^{-2} d\xi \\
&= - \left[\frac{1}{x_i - \xi_j - \frac{l_j}{2}} - \frac{1}{x_i - \xi_j + \frac{l_j}{2}} \right] \quad (4.2c)
\end{aligned}$$

where $l_j = \frac{1}{N}$ (step size)

Writing (4.1) in following form

$$u_i^2 - 2u_i + 2\bar{u}_{Li} - 2 \sum_{j=1}^N \varepsilon_{ij} \frac{u_j^2}{2} + 2 \sum_{j=1}^N \delta_{ij} u_j = 0$$

$$i = 1, 2, \dots, N \quad (4.3)$$

Now to execute (4.3) numerically, the value of u versus x is to be considered as divided up into a number of equally or unequally spaced strips, over which u is assumed to be constant in steps. If l_j is taken to represent the width of the j th strip of the divisions into which x -axis is partitioned, ξ_j represents the mid-point of this j th strip and u_j stands for the ordinate corresponding to the height of this strip, then at this particular j th step e_{ij} and δ_{ij} are defined as in (4.2a) and (4.2b).

Thus a set of non-linear algebraic equations (4.3) can be solved by different iteration schemes. The solutions to these equations can also be obtained by the use of artificial viscosity in various numerical calculation methods and one of these methods which ^{we} use here is the method of parametric differentiation. This approach is due to Norstrud (11) applied to nonlifting problem.

First we shall discuss the method of iteration scheme for present nonlifting problem and then the parametric differentiation method for the same.

4.2 METHOD OF ITERATION

The integral equation (3.33) for perturbation velocity can be solved by the method of iteration. To do so we arrange (3.33) as follows.

$$u(x,0) = \bar{u}_L(x,0) + \frac{u^2}{4}(x,0) - I_\tau(x,0) + u_s(x,0) \quad (4.4)$$

where $I_\tau = (I - \frac{u^2}{4})$

and $I = - \int_{-\infty}^{\infty} \frac{u^2(\xi,0)}{2b(\xi)} E(Z) d\xi$

This can be further expressed in the form of a quadratic equation

$$u^2(x,0) - 4u(x,0) + 4\{\bar{u}_L(x,0) - I_\tau(x,0) + u_s(x,0)\} = 0 \quad (4.5)$$

Equation (4.5) has the following roots

$$u(x,0) = 2[1 \pm \{1 - (\bar{u}_L(x,0) - I_\tau(x,0) + u_s(x,0))\}^{\frac{1}{2}}] \quad (4.6)$$

Since the flow is high subsonic for which $u(x,0) < 2$, we retain only the negative sign before the radical in (4.6).

Thus we have

$$u(x,0) = 2[1 - \{1 - (\bar{u}_L(x,0) - I_\tau(x,0) + u_s(x,0))\}^{\frac{1}{2}}] \quad (4.7)$$

First of all, \bar{u}_L is computed numerically.

Then, equation (4.7) is operated for $u(x,0)$ by neglecting integrals $I_\tau(x,0)$ and $u_s(x,0)$. Now, with this computed value of $u(x,0)$ the integral $I_\tau(x,0)$ is computed and substituted in (4.7), keeping integral $u_s(x,0)$ equal to zero to get new value of $u(x,0)$. With this new value of

$u(x,0)$ the integral $I_\tau(x,0)$ is computed again and this computed value is substituted in (4.7), keeping $u_s(x,0)$ equal to zero. The above procedure is repeated till the value of $u(x,0)$ converges. Then with this converged value of $u(x,0)$ the integral $u_s(x,0)$ is computed and put in (4.7), that gives the final value of $u(x,0)$.

4.3 METHOD OF PARAMETRIC DIFFERENTIATION

The method of parametric differentiation is applied for solving the non-linear algebraic equation (4.3) for the unknown u_i (20). To do so a parameter $\bar{\mu}$ is introduced as follows

$$F_i(u_i(\bar{\mu}), \bar{\mu}) = u_i - \bar{u}_{L_i} - \bar{\mu} \left[\frac{1}{2} u_i^2 - \sum_{j=1}^N \epsilon_{ij} u_j^2 + \sum_{j=1}^N \delta_{ij} u_j \right] = 0 \quad (4.8)$$

$$i = 1, 2, \dots, N$$

By differentiating (4.8) with respect to the parameter $\bar{\mu}$, we get a system of first order non-linear ordinary differential equations. Considering \bar{u}_{L_i} independent of $\bar{\mu}$, because \bar{u}_{L_i} is solution of (4.8) at $\bar{\mu} = 0$ and unknown $\bar{u}_i = u_i(\bar{\mu})$, we obtain the set of ordinary differential equations as

$$\begin{aligned}
\frac{du_i}{d\bar{\mu}} = & \frac{1}{(1 - \bar{\mu} u_i)} \left[\frac{1}{2} u_i^2 - \sum_{j=1}^N \epsilon_{ij} \left(\frac{u_j^2}{2} + u_j \frac{du_j}{d\bar{\mu}} \right) \right. \\
& \left. + \sum_{j=1}^N \delta_{ij} \left(u_j + \frac{du_j}{d\bar{\mu}} \right) \right] \\
& i = 1, 2, \dots, N
\end{aligned} \tag{4.9}$$

The unknown vector u_i can be determined from differential equations as the solution to the defined Cauchy's problem at $\bar{\mu} = 1$, with the initial vector solution

$$u_i = \bar{u}_{L_i} \quad \text{at} \quad \bar{\mu} = 0 \tag{4.10}$$

The condition for a unique solution of system (4.9) in the range $0 \leq \bar{\mu} \leq 1$ is the nonvanishing of the functional determinant or Jacobian of $F_i[u_i(\bar{\mu}), \bar{\mu}]$ with respect to u_i for fixed $\bar{\mu}$. Jacobian matrix of the system is given by

$$J(u_1, u_2, \dots, u_n) = \frac{\partial(F_1, \dots, F_n)}{\partial(u_1, \dots, u_n)} \tag{4.11}$$

and (4.11) is positive definite under the condition that the elements on the principal diagonal are positive, i.e.,

$$(1 - \bar{\mu} u_i) > 0$$

$$u_i < \bar{\mu}^{-1}, \quad i = 1, 2, \dots, N$$

For a certain value of $\bar{\mu} \geq \max[u_i^{-1}]$ however Jacobian matrix becomes singular and the solution curve of Cauchy problem

can split into two or more solutions. Such a point $\bar{\mu} = \bar{\mu}^*$ in the interval $0 \leq \bar{\mu} \leq 1$ for which $\det J(u_1, u_2, \dots, u_N) = 0$ can be treated as bifurcation point and the associated solution $u_i^* = u_i(\bar{\mu}^*)$ is designated as the bifurcation solution.

After obtaining numerically a unique and real solution $u_i = u_i(\bar{\mu})$ for (4.9) at value $\bar{\mu} \leq \bar{\mu}^* < 1$, which represents within some given error bound, the best possible approximation to the condition ^{of} minimum bifurcation, the next step in the integration of (4.9) will involve crossing of singular Jacobian matrix. Therefore a continuous dependence of the solution on the initial data is no longer possible. Then, method of steepest descent is applied for the system of algebraic equation (4.8). For continuous flows the initial values for the steepest descent method are those at which the Jacobian matrix becomes singular. From the bifurcation point the iteration by steepest descent method is carried upto $\bar{\mu} = 1$ to get final velocity distribution.

In the present case, Hamming's predictor-corrector method in conjunction with fourth order Runge-Kutta starter has been employed to integrate the set of differential equations.

CHAPTER 5

COMPUTATIONAL DETAILS, RESULTS AND DISCUSSION

5.1 INTRODUCTION

The computational details for the methods used in solving the system of equations (4.3) are given in Chapter 4. Results are computed and compared for NACA 0012 airfoil at different free stream Mach numbers by the method of iteration and parametric differentiation. The leading edge correction slightly lowers the value of linear coefficient of pressure at the leading edge of the airfoil Figure 5.

5.2 METHOD OF ITERATION

The flow chart is shown in Figure 3. Listing of the computer program is given in Appendix B. Definition of the variables used in the program is given in the listing. The slope of the airfoil is denoted by F . The subroutine KARMAN calculates the linear velocity distribution $UBAR$. This linear velocity is modified by applying leading edge correction and used to find the first approximation of U . Then, the subroutine LIPMAN is called, which uses the above U as the initial value and calculates the inviscid non-linear effects by iterating each new value of U until

CENTRAL LIBRARY

Acc. No. **A 51160**

convergence is achieved. The subroutine GLUERT uses the converged inviscid value of U and calculates the final values of U in boundary layer flow.

5.3 METHOD OF PARAMETRIC DIFFERENTIATION

The listing of the developed program for the problem under consideration is given in Appendix C. The flow chart describing the main steps of the computer program is shown in Figure 4. The different variables used for computation are defined in the program listing. The equation for NACA 0012 airfoil is denoted by $Y(\Lambda)$. The linear velocity distribution UBR , is calculated separately and fed to the main program.

For applying the Hamming's predictor-corrector method the initial values are calculated using the Runge-Kutta method. A step size H is assumed and the initial conditions for the Runge-Kutta method are taken at $\mu = 0$, $U = UBR$. The subroutine `FUNC` calculates the velocity derivative F . In the subroutine `FUNC`, the subroutine `MITAL` is called which calculates the influence coefficient E . In the Runge-Kutta method, wherever the velocity derivative is required, the subroutine `FUNC` is called. In the Hamming's predictor-corrector method, the solution

vector USP is first predicted. The solution vector USP is then modified using the corrector formula. A convergence test is applied after each step to ensure that the values are within the prescribed error bounds. After calculating the final velocity distribution USN, at different AMEW, a check is applied for the Jacobian matrix.

5.4 RESULTS AND DISCUSSION

Results are obtained for the NACA 0012 airfoil at Mach numbers of 0.4, 0.5, 0.6, 0.7 and 0.72. It is observed that the results obtained in boundary layer flow are higher than that for a non-linear inviscid flow. Figures 8,9,10,11 and Figure 12, show the comparison of the results obtained for coefficient of pressure.

The presence of a boundary layer on the surface of the airfoil produces a distortion of the streamlines close to the surface equivalent to a change in the thickness distribution. Consequently, the perturbation velocity of the outer inviscid flow on the modified surface of the airfoil, increases. This explains as to why the coefficient of pressure is more negative for the boundary layer flow as compared to that of the non-linear inviscid flow. It is also observed that the difference between the two results

are more pronounced at higher Mach numbers because the displacement thickness, increases with an increase in the perturbation velocity.

The results obtained by the method of parametric differentiation and the method of iteration Figure 7 agree except near the leading edge of the airfoil at low Mach numbers. This is because the number of steps taken in the method of iteration is twice that taken in the method of parametric differentiation. The slope of the airfoil, at the leading edge, changes rapidly and hence the difference in the number of steps taken produces an appreciable divergence in the results.

The calculations were performed on the computer system IBM 7044. The order of magnitude of the computer time used for getting the final results for the methods of iteration and parametric differentiation are given below:

Method of iteration	3-5 minutes
Method of parametric differentiation	5-8 minutes

5.5 CONCLUSIONS

To conclude, we observe that the presence of a boundary layer on the surface of the airfoil increases the negative coefficient of pressure as compared to that

for the non-linear inviscid flow. The method of iteration, for calculating the problem of boundary layer flow past an airfoil at a high subsonic speed, is better suited than the method of parametric differentiation as the computer program is simple to construct and the computational times involved are less.

REFERENCES

1. Ashley, H., and Landahl, M., "Aerodynamics of Wings and Bodies", Addison-Wesley Publishing Company, Inc. Reading, Massachusetts
2. Anderson, W.J., and Fung, W.C., "The Effect of An Idealised Boundary Layer on the Flutter of Cylindrical Shells in Supersonic Flow", GALCIT Structural Dynamics Report, SM 62-49, Dec., 1962
3. Benjamin, T.B., "Shearing Flow Over a Wavy Boundary", J. Fluid Mech. 6, 1959
4. Brebner, G.G., Bagley, J.A., "Pressure and Boundary Layer Measurements on a Two Dimensional Wing at Low Speed", A.R.C., R. & M. 2886, 1952
5. Ferrari, C., and Tricomi, F.G., "Transonic Aerodynamics", Academic Press, New York and London, 1968
6. Gullstrand, T.R., "The Flow Over Symmetric Aerofoils Without Incidence at Sonic Speed", KTH Aero. TN 24, 1952
7. Inger, G.R., and Williams, "Subsonic and Supersonic Boundary Layer Flow Past Wavy Wall", AIAA J. 10, No. 5, 1972
8. Lighthill, M.J., "Supersonic Flows Without Separation", Quart. J. Mech. 3, 303, 1950
9. Lees, L., and Reeves, B.L., "Supersonic Separated and Reattaching Laminar Flows", AIAA J. 2, No. 11, 1964
10. Nixon, D., and Hancock, G.J., "High Subsonic Flow Past A Steady Two Dimensional Aerofoil", C.P. No. 1280, 1974
11. Norstraud, H., "The Transonic Airfoil Problem With Embedded Shocks", The Aeronautical Quarterly, Vol. XXIV, May 1973
12. Ostwatitsch, K., "Die Geschwindigkuto-verteilung bei lokolen Überschallgebieten an flachen Profilen-Seitzchrift fier Augewandte Mathematik und Mechanik Bd 30 NR 1/2, 1950

13. Schlichting, H., "Boundary Layer Theory", McGraw-Hill, Inc., 1960
14. Stratford, B.S., and Beavers, G.S., "The Calculation of the Compressible Turbulent Boundary Layer in an Arbitrary Pressure Gradient", ARC RM 3207; 1959
15. Spreiter, J.R., and Alksne, A., "Theoretical Prediction of Pressure Distribution on Non-lifting Aerofoils at High-Subsonic Speeds", NACA TN 3096; 1954
16. Thwaites, B., "Incompressible Aerodynamics", Clarendon Press, Oxford, 1961
17. Tsien, H.S., "Symmetrical Joukowski Airfoils in Shear Flow", Quarterly of Applied Mathematics, Vol. 1, 1943
18. Ventres, C.S., "Shear Flow Aerodynamics: Lifting Surface Theory", AIAA Journal, Vol. 13, No. 9, Sept. 1975
19. Yates, John, E., "Linearized Integral Theory of the Viscous Compressible Flow Past a Wavy Wall", A.R.A.P. Report No. 177, 1972
20. Yakovlev, M.N., "The Solutions of Systems of Non-linear Equations by A Method of Differentiation With Respect to A Parameter", USSR Computational Mathematics and Mathematical Physics, Vol. 4, 1964
21. Zeydel, E.F.E., "Study of the Pressure Distribution on Oscillating Panels in Low Supersonic Flow with Turbulent Boundary Layer", NASA CR-691, 1967

APPENDIX A

SINGULARITY CORRECTIONS AT LEADING EDGE OF THE AIRFOIL

One main disadvantage of the linear theory is that the solution of $u_D(x,0)$ as given by (3.32a); is singular at the leading edge. It implies that a more accurate solution to that given by linear theory should be used in the region of the leading edge, preferably without any singular behaviour.

Now consider the governing differential equation
(2.13)

$$(1 - M_\infty^2)\Phi_{XX} + \Phi_{YY} = (\gamma + 1)M_\infty^2 \Phi_X \Phi_{XX} \quad (A.1)$$

with boundary condition on the surface of the airfoil (16)

$$\frac{\Phi_Y(X,0\pm)}{1 + \Phi_X(X,0\pm)} = \pm \frac{df}{dX} \quad (A.2)$$

where f represents the surface of the airfoil. Applying the transformation (3.1) to (A.2), we get

$$\frac{\phi_Y(x,0\pm)}{\frac{k}{\beta_\infty^2} + \phi_X(x,0\pm)} = \pm \frac{1}{\beta_\infty} \frac{df}{dx} \quad (A.3)$$

where $k = (\gamma + 1) M_\infty^2$ and $\beta_\infty = \sqrt{1 - M_\infty^2}$

Now from (2.15b) together with the transformation (3.1), we get at the surface of the airfoil

$$\bar{q}(x, 0_{\pm}) = \left[\frac{k}{\beta^2} + u_L(x, 0_{\pm}) \right] \left[1 + \left(\frac{1}{\beta^2} \frac{df}{dx} \right)^2 \right]^{\frac{1}{2}} \quad (\text{A.4})$$

The exact flow remains finite everywhere so that at the nose of the airfoil

$$u_L(x, 0_{\pm}) \rightarrow -\frac{k}{\beta_{\infty}^2} \text{ as } \pm \frac{df}{dx} \rightarrow \infty$$

Then (A.4) can be written in the form

$$\bar{q}(x, 0_{\pm}) = \frac{\left[\frac{k}{\beta_{\infty}^2} + u_L(x, 0_{\pm}) \right] \left[1 + \frac{1}{\beta_{\infty}^2} \frac{df}{dx} \right]}{\left[1 + \left(\frac{1}{\beta_{\infty}^2} \frac{df}{dx} \right)^2 \right]^{\frac{1}{2}}} \quad (\text{A.5})$$

where both the numerator and the denominator tend to infinity at nose.

If the standard linearised solution $u_L(x, 0)$ given by (3.32a) is to be used as an approximation to modified linear velocity $\bar{u}_L(x, 0_{\pm})$ and since this linearised solution already incorporates an infinity at the leading edge then an approximation to $\bar{q}(x, 0_{\pm})$ is taken to be

$$\bar{q}(x, 0_{\pm}) = \frac{\frac{k}{\beta^2} + u_L(x, 0_{\pm})}{\left[1 + \left(\frac{\beta_{\infty}^2}{k} \frac{df_t}{dx} \right)^2 \right]^{\frac{1}{2}}} \quad (\text{A.6})$$

It is noted that only the thickness term is retained in (A.6). This is done for two reasons, first it is only the thickness term which gives necessary infinity at leading edge, second it is necessary to preserve the same denominator for both the upper and lower surfaces to ensure that Kutta condition at the trailing edge is satisfied, since $u_L(x, 0_{\pm})$ already satisfies Kutta condition.

An approximation to the $\bar{q}(x, 0_{\pm})$ may be written as

$$\bar{q}(x, 0_{\pm}) = \frac{k}{\beta_{\infty}^2} + \bar{u}_L(x, 0_{\pm}) \quad (\text{A.7})$$

where $\bar{u}_L(x, 0_{\pm})$ can be regarded as the linear solution modified for leading edge corrections. Combining (A.6) and (A.7), we obtain

$$\bar{u}_L(x, 0_{\pm}) = \frac{\frac{k}{\beta_{\infty}^2} + u_L(x, 0_{\pm})}{\left[1 + \left(\frac{\beta_{\infty}^2}{k} \frac{df_t}{dx}\right)^2\right]^{\frac{1}{2}}} - \frac{k}{\beta_{\infty}^2} \quad (\text{A.8})$$

AE-1947-M-DOG-BOVA 51160

Date Slip **A 51160**

This book is to be returned on the
date last stamped.

This image shows a blank sheet of white paper with horizontal ruling lines. A single vertical line runs down the center of the page, creating two equal-width columns. The horizontal lines are evenly spaced and extend across the entire width of the paper, including both columns. There is no handwriting or other markings on the page.

CD 6 72.9